ChemPlusChem

Research Article
doi.org/10.1002/cplu.202200284

Chemistry Europe
European Chemical Societies Publishing

www.chempluschem.org

Special Collection

Phosphinine Selenide: Noncovalent Interactions with Organoiodines and Elemental Iodine, and Reactivity towards Potassium Cyanide

Jinxiong Lin,[a] Nathan T. Coles,[a, b] Manuela Weber,[a] and Christian Müller*[a]

Dedicated to Prof. László Nyulászi on the occasion of his 65th birthday

A co-crystalline adduct consisting of a phosphinine selenide and an organohalide was obtained by slow evaporation of the solvent from a mixture of 2,6-bis(trimethylsilyl)phosphinine selenide and 1,4-diiodotetrafluorobenzene (1,4-TFDIB). The crystallographic characterization of the product shows π-π stacking, F···H hydrogen bonding between 1,4-TFDIB and the phosphinine selenide, as well as F···F interactions between 1,4-TFDIB molecules. Moreover, the phosphorus heterocycle could be crystallized with diiodine to form a 1:1 adduct. The $d_{(I–I)}$ distance in this compound is 2.8475(3) Å, which is shorter than the corresponding one in triphenylphosphine selenide diiodide, reflecting the weaker net-donor power of the phosphinine selenide towards diiodine. The phosphinine selenide could also be used as a selenium transfer reagent to generate KSeCN from KCN.

Introduction

Since the first synthesis of phosphine selenides ($R_3P{=}Se$, R = alkyl, aryl), a vast amount of reports concerning their application in several fields of chemical research have been published in literature.[1] In general, trivalent phosphines readily react with grey selenium to form quantitatively phosphine selenides, which are thermodynamically and kinetically rather stable compounds.[2] Consequently, the selenium atom can be used as a protecting group, which can be removed again by different methods.[3] Moreover, the ^1J coupling between the ^{31}P and ^{77}Se nucleus provides valuable information on the basicity of the trivalent phosphorus atom, which is of fundamental importance when applying organophosphorus compounds as ligands in homogeneous catalysis.[4] Interestingly, the selenium atom in triphenylphosphine selenide ($Ph_3P{=}Se$, **1**) shows a high affinity towards organoiodines, which often results in the formation of co-crystalline adducts with non-covalent halogen bonding interactions. Pennington and co-workers have reported on cocrystals, that display halogen bonding, by combining **1** with 1,2-diiodotetrafluorobenzene (1,2-TFDIB), 1,4-diiodotetrafluorobenzene (1,4-TFDIB, **2**), and tetraiodoethylene (TIE), respectively (Scheme 1). In this way finite adducts, chains and two-dimensional layers could be assembled.[5] 1,4-TFDIB has been extensively investigated as a tool in cocrystal formation as the polarizable iodine atoms attached to the aromatic ring lead to the presence of σ-holes. This, in turn, facilitates the formation of halogen bonds. On the other hand, π-hole is generated at the π-surface of the aryl-ring, due to the presence of highly electronegative fluorine atoms, that cause an electron-deficient core.[6] Halogen bonding as a non-covalent interaction is a

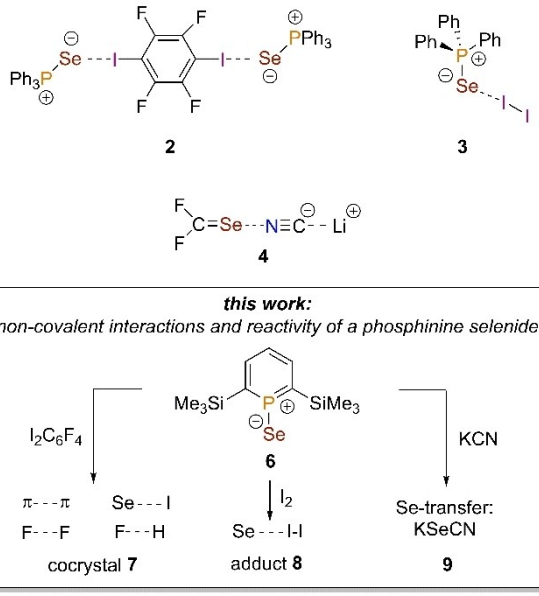

Scheme 1. Adducts of $Ph_3P{=}Se$ with 1,4-TFDIB (**2**) and I_2 (**3**). Interaction of LiCN with $F_2C{=}Se$ (**4**) and brief summary of this work.

[a] J. Lin, Dr. N. T. Coles, M. Weber, Prof. Dr. C. Müller
Institut für Chemie und Biochemie
Freie Universität Berlin
Fabeckstr. 34/36, 14195 Berlin (Germany)
E-mail: c.mueller@fu-berlin.de
[b] Dr. N. T. Coles
School of Chemistry
University of Nottingham
University Park Campus, NG7 2RD Nottingham (UK)

Supporting information for this article is available on the WWW under https://doi.org/10.1002/cplu.202200284

Special Collection *Part of a Special Collection: "From Light to Heavy: Advancing the Chemistry of Pnictogen Compounds"*

valuable instrument in understanding the association of molecules in a crystalline environment.[7] This topic recently attracted a lot of attention, for instance, for the synthesis of diverse crystalline forms,[8] the development of photoluminescent materials,[9] the construction of stoichiomorphic donor-acceptor aggregates and the exploration of the nature and energetics of intermolecular interactions.[10,11]

Besides the formation of halogen bonding using organoiodine compounds, phosphine selenides can also form charge-transfer complexes with dihalogens. The first examples were reported by Zingaro and co-workers in 1960, who showed that $R_3P{=}Se$ (R = alkyl or aryl) can form 1:1 adducts with I_2 (**3**), IBr and ICl in CCl_4.[12] Godfrey and co-workers characterized crystallographically several phosphine selenide dihalides and showed, that the donor power of the selenium atom in $R_3P{=}Se$ towards diiodine is sensitive to the nature of the R groups.[13]

Also, chalcogen bonds with nitrogen bases are known. This type of noncovalent Se···N interaction plays a prominent role with respect to molecular recognition, biological systems as well as crystal engineering.[14] In this case, the σ-hole at the selenium atom can interact with the lone pair of nitrogen-based compounds (**4**, Scheme 1).[15]

Our group recently reported on the first synthesis of a phosphinine selenide (**6**, Scheme 1).[16] In contrast to classical phosphines, the selenation of phosphinines is rather challenging as the phosphorus atom in the aromatic phosphorus heterocycle shows a very weak basicity along with a poor nucleophilicity. These characteristics severely hindered the reaction with grey selenium. However, the electronic properties of phosphinines can be drastically influenced by introducing strongly electron-donating Me_3Si-substituents to the heterocyclic ring. In this way, it was possible to react the bis-$SiMe_3$-substituted phosphinine **5** with red selenium to the corresponding phosphinine selenide, albeit the desired product could finally not be characterized crystallographically. Interestingly and similar to **4** (Scheme 1), the phosphinine selenide **6** is expected to be a multifunctional molecule, with a σ-hole at the selenium atom, a π-hole at the phosphorus atom (energetically low-lying LUMO) as well as two lone-pairs perpendicular to one another with a high *p*-character at the selenium atom. This is also reflected in the corresponding electrostatic potential plot of **6** (Figure 1) and indicates that the phosphinine selenide should have the potential to form adducts with organoiodine compounds as well as with halogens and nitrogen bases and that the formation of co-crystalline adducts can be expected.[16] These qualitative considerations prompted us to investigate the reactivity of phosphinine selenide **6** towards organoiodines, dihalogens as well as CN^- in more detail.

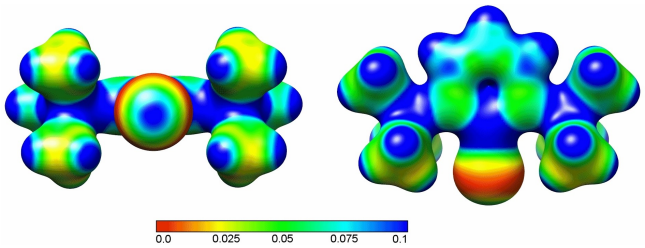

Figure 1. Electrostatic potential plot of **6** calculated at B3LYP–D3/def2-TZVP level of theory. The electrostatic potential (in a.u.) is mapped on electron density isosurfaces of 0.02 e/au^3 (in accordance to ref. [16]).

Results and Discussion

As 1,3,5-trifluoro-2,4,6-triiodobenzene (TFTIB), 1,2-TFDIB, 1,4-TFDIB, as well as TIE have been used successfully in the formation of co-crystals with $Ph_3P{=}Se$ and Ph_3P before,[5,8] we started a systematic study these organoiodines in combination with phosphinine selenide **6**. At first, an equimolar solution of TFTIB and **6** in different solvents (see Supporting Information) was prepared at $T = -30\,^{\circ}C$ and the solvent was slowly evaporated at room temperature. Colorless crystals were obtained, which turned out to be the starting material TFTIB. With 1,2-TFDIB and TIE, only viscous oils were obtained with **6**. When using a combination of 1,4-TFDIB and **6** in deuterated dichloromethane as solvent, the ^{31}P NMR spectrum of the mixture shows a signal at δ(ppm) = 168.4 with ^{77}Se-satellites, which is identical to the pure phosphinine selenide **6**.[16] However, when using a mixture of dichloromethane and *n*-pentane, single crystals, suitable for X-ray diffraction, could be obtained by slow evaporation of the solvent mixture.

The crystallographic characterization of the product **7** reveals indeed the presence of a co-crystalline adduct that crystallizes in the centrosymmetric monoclinic space group $P2_1/c$. The unit cell consists of four molecules 1,4-TFDIB and four molecules of **6** (Figure 2), while the asymmetric unit contains two half molecules of crystallographically different molecules of 1,4-TFDIB. Figure 2 represents the first structurally characterized phosphinine selenide.

The P(1)–Se(1) bond length of 2.083(1) Å is slightly shorter than the one found in the co-crystalline product of 1,4-TFDIB and $Ph_3P{=}Se$ (2.127(2) and 2.107(2) Å).[5] As expected, the Se atom lies very close to the axis defined by the P(1) and C(3) atoms (Se(1)–P(1)–C(3): 178.64°), while the phosphorus heterocycle is essentially planar with a P(1)–C(1)–C(2)–C(3) torsion angle of 0.2°. This situation may contribute to π-π stacking. In fact, the phosphorus heterocycle and the closest 1,4-TFDIB

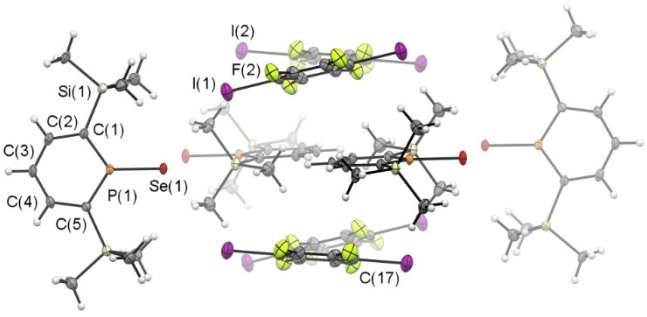

Figure 2. Molecular structure of phosphinine selenide···1,4-TFDIB adduct **7** in the crystal (unit cell). Displacement ellipsoids are shown at the 50% probability level. Selected bond lengths (Å) and angles (°): Se(1)–P(1): 2.083(1), P(1)–C(1): 1.721(5), P(1)–C(5): 1.715(5), C(1)–C(2): 1.414(7), C(2)–C(3): 1.387(8), C(3)–C(4): 1.390(8), C(4)–C(5): 1.396(7), C(1)–P(1)–C(5): 111.8(3).

molecule show nearly an offset-stacked geometry with *d*(C17···centroid(**6**) = 3.852 Å and *d*(C3-centroid(1,4-TFDIB) = 3.634 Å. The C–C bond distances in the phosphinine selenide are very similar to the ones observed in a 2,6-bis-Si(CH_3)$_3$-substituted phosphinine sulphide, reported by Le Floch and co-workers.[17] The same is observed for the P(1)–C(1) and P(1)–C(5) bond lengths (1.721(5) and 1.715(5) Å, respectively) as well as for the C(1)–P(1)–C(5) angle of 111.75°.

A closer look to the packing of the molecules in the crystal of **7** reveals further distinct features (Figure 3). The iodine atoms of one of the 1,4-TFDIB molecules show potential I(2)···Se(1) contacts to two different phosphinine selenides, with an interatomic distance of $d_{(I\cdots Se)}$ = 3.8730(7) Å (Figure 3, blue dotted line). This value is significantly longer than the one found for the cocrystal consisting of Ph_3P=Se and 1,4-TFDIB ($d_{(I\cdots Se)}$ = 3.4944(11), 3.6841(12), 3.4224(13) Å) and almost equal to the sum of the van der Waals radii of selenium and iodine (3.91 Å).[5,18] The second molecule of 1,4-TFDIB has a distance of I(1)···Se(1) of 4.0216(7) Å, which is clearly outside the sum of the van-der-Waals radii and is not to be considering interacting. Moreover, the P=Se···I angle is with 130.69(4)° considerably larger than the one found in Ph_3P=Se···1,4-TFDIB (113.01(7)°, 88.90(6)°, and 112.60(7)°). The C(17)–I(2)–Se(1) angle of 143.71° deviates substantially from linearity. Consequently, only a weak interaction of the selenium atom with the σ-hole of 1,4-TFDIB should be considered. The four fluorine atoms of 1,4-TFDIB form short F···F contacts of 2.692(6) and 2.757(6) Å with neighboring 1,4-TFDIB molecules (Figure 3, red dotted lines), as well as two F···H hydrogen bonds with adjacent phosphinine selenides ($d_{(F\cdots H)}$ = 2.579 Å and 2.623 Å, Figure 3, green dotted lines). Overall we assume that the co-crystal **7** is primarily held together by F···F and F···H interactions as well as π-π stacking, with only slight contributions by Se···I contacts.

It is well known that Ph_3P=Se can form charge-transfer (CT) adducts when combined with stoichiometric amounts of an appropriate dihalogen or interhalide compounds.[13] Upon addition of Br_2 to **6** in dichloromethane, however, the formation of several products was observed by means of $^{31}P\{^1H\}$ NMR spectroscopy, even at T = −30 °C. We anticipate that the rather reactive bromine reacted unselectively with the unsaturated phosphorus heterocycle. The same was observed when the interhalide compounds IBr and ICl, respectively, were used. Nevertheless, when I_2 was added to **6** at room temperature in dichloromethane, the $^{31}P\{^1H\}$ NMR spectrum revealed a single resonance at δ(ppm) = 162.0, which is only slightly shifted compared to the starting material (δ(ppm) = 170.3). Additionally, the $^1J_{P,Se}$ coupling constant decreased numerically from 883 Hz to 833 Hz. Much to our delight, the slow evaporation of the solvent at T = −30 °C afforded large dark red crystals, which were suitable for single crystal X-ray diffraction.

The crystallographic characterization reveals, that an I_2 adduct of **6** has indeed been formed. The molecular structure of the new compound (**8**) and its packing in the solid state is depicted in Figure 4, along with selected bond lengths and angles.

The I(1)–I(2) bond length in **8** is with 2.8475(3) Å slightly shorter compared to Ph_3P=Se···I_2, while the distance $d_{(Se-I)}$ is with 2.8585(3) Å somewhat longer than in the triphenylphos-

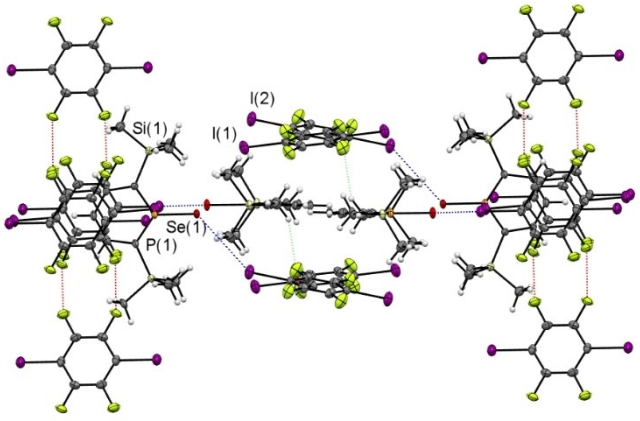

Figure 3. Overview of molecular packing in the cocrystal of **7**. 1,4-TFDIB molecule is involved in I···Se interactions (blue), short F···H contacts with two neighboring phosphinine selenides (green), and short F···F short contacts with neighboring 1,4-TFDIB molecules (red).

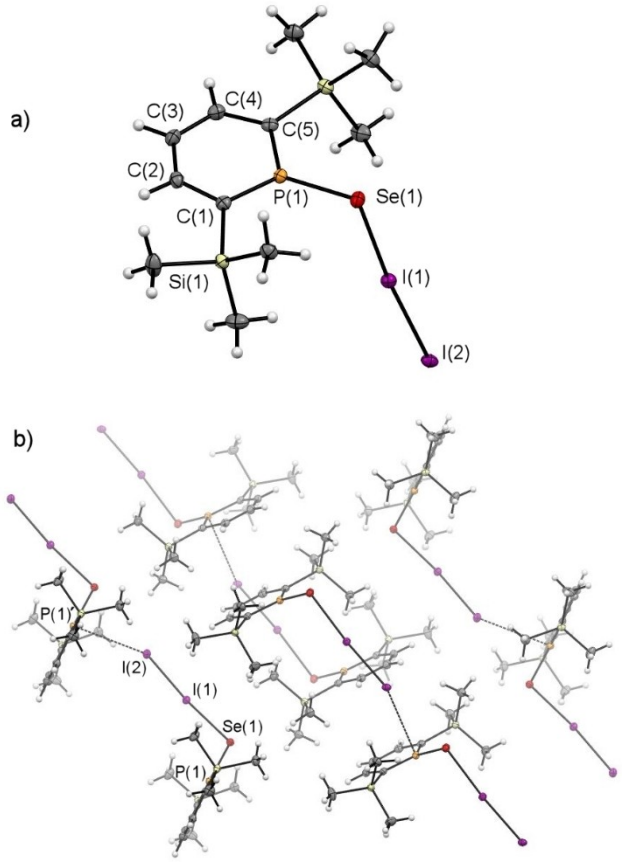

Figure 4. Molecular structure of phosphinine selenide-diiodide adduct **8** in the crystal and packing of **8** in the solid state. Displacement ellipsoids are shown at the 50% probability level. Prime (') donates a symmetry equivalent atom generated using the following equation: 1 + x, + y, + z. Selected bond lengths (Å) and angles (°): I(1)–Se(1): 2.8585(3), I(1)–I(2): 2.8475(3), Se(1)–P(1): 2.1243(6), P(1)–C(1): 1.709(2), P(1)–C(5): 1.705(2), C(1)–C(2): 1.401(2), C(2)–C(3): 1.395(2), C(3)–C(4): 1.395(3), C(4)–C(5): 1.399(2), I(2)–P(1)': 3.6853(5). Se(1)–I(1)–I(2): 174.500(15); I(1)–Se(1)–P(1): 105.85(2), C(1)–P(1)–C(5): 113.81(8).

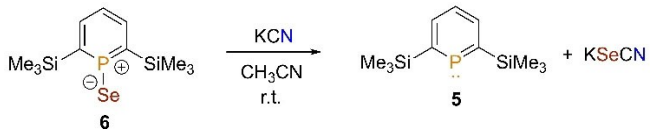

Scheme 2. Reaction of phosphinine selenide **6** with KCN in acetonitrile.

phine derivative ($d_{(I–I)}$: 2.881(2) Å; $d_{(Se–I)}$: 2.803(3) Å; $d_{(I–I)}$ in I_2: 2.71 Å). This can be attributed to the smaller polarization of the Se(1)–I(1) bond in **8**. Moreover, the P(1)–Se(1)–I(1) bond angle in **8** is with 105.85(2)° very similar with respect to $Ph_3P{=}Se{\cdots}I_2$ (106.0(1)°). This is in line with the donation of electron density from one of the non-bonding *p*-orbitals at the selenium atom to the σ-hole of the I_2 molecule. The Se(1)–I(1)–I(2) moiety is essentially linear (174.500(15)°), which is consistent with other crystallographically characterized charge-transfer complexes of diiodine (Scheme 1).[13]

Additionally, the P(1)–Se(1) bond in **8** is with 2.1243(6) Å considerably longer with respect to **7** (2.083(1) Å). Also this observation is in line with earlier computational studies on phosphinine selenides, which show, that the two non-bonding *p*-orbitals at the selenium atom are involved in backdonation to σ*(P–C) and π*(P–C) orbitals.[16] Consequently, also the bond lengths P(1)–C(5) (1.705(2) Å) and P(1)–C(1) (1.709(2) Å) are shorter in **8** with respect to **7** (1.721(5), 1.715(5) Å).

Additionally, I(2) has a short contact of 3.6853(5) Å to the phosphorus atom P(1)' of a neighbouring phosphinine selenide (Figure 4b), which is significantly shorter than the sum of the van-der-Waals radii of these atoms. This is perfectly in line with the presence of a formal positive charge at the phosphorus atom.

As the σ-hole at the selenium atom of **6** (Figure 1) is in fact larger than the corresponding one in $Ph_3P{=}Se$, we anticipated that the rather nucleophilic CN^- anion might form a strong Se···NCK bond. Compound **6** was thus reacted with KCN in acetonitrile at room temperature (Scheme 2).

Upon slow evaporation of the solvent, single crystals, suitable for X-ray diffraction, were obtained. Much to our surprise, we found that KSeCN had been formed, rather than the expected adduct of the type **6**···NCK (Figure S10). This polymorph of KSeCN can be found in the Cambridge Crystallographic Data Center.[19] Apparently, **6** serves as a very good selenium-transfer reagent, rather than participating in non-covalent interactions.

Conclusion

In conclusion, we have structurally characterized for the first time the phosphinine selenide (**6**) in form of a co-crystalline adduct with the organoiodine 1,4-TFDIB (**7**). The molecular structure of **7** in the solid state is stabilized by several non-bonding interactions, including π-π stacking, hydrogen bonding, F–F– and Se–I interactions. This demonstrates that phosphinine selenides can be used efficiently as a multifunctional molecule for crystal design. Moreover, we could show that the phosphinine selenide also forms an adduct with diiodine *via* interaction of one of the selenium lone-pairs with the σ-hole at the I_2 molecule, as confirmed by single crystal X-ray diffraction. The iodine molecule shows an additional contact with the phosphorus atom of a neighboring phosphinine selenide, which carries a formal positive charge. Moreover, it turned out that the phosphinine selenide acts as an efficient selenium transfer reagent as it reacts selectively with KCN towards KSeCN.

Experimental Section

General Remarks: All reactions were performed under argon in oven-dried glassware using modified Schlenk techniques unless otherwise stated. All common solvents and chemicals were commercially available and were used without further purification. All dry or deoxygenated solvents were prepared using standard techniques or an MBraun solvent purification system. 2,6-Bis(trimethylsilyl)phosphinine selenide (**6**) was prepared according to the literature.[16] The ^{1}H, ^{13}C{^{1}H}, ^{19}F, ^{29}Si{^{1}H}, ^{31}P, ^{31}P{^{1}H} and ^{77}Se {^{1}H} NMR spectra were recorded on a JEOL ECX400 (400 MHz) and a Bruker Avance 600 (600 MHz) spectrometer and all chemical shifts are reported relative to the residual resonance in the deuterated solvents. The HRMS ESI mass spectra were measured on an Agilent 6210 ESI-TOF.

Single crystal X-ray diffraction: Low-temperature and room-temperature X-ray diffractometry was performed on a Bruker-AXS X8 Kappa Duo diffractometer with *IμS* micro-sources, performing ϕ- and ω-scans. The data were collected using a Photon 2 CPAD detector with Mo K_α radiation ($\lambda = 0.71073$ Å). The structures were solved by dual-space methods using SHELXT[20] and refined against F^2 on all data by full-matrix least squares with SHELXL-2017[21] following established refinement strategies[22]. The program Olex2[23] was also used for refinement. All non-hydrogen atoms were refined anisotropically. All hydrogen atoms were included into the model at geometrically calculated positions and refined using a riding model. The isotropic displacement parameters of all hydrogen atoms were fixed to 1.2 times the *U*-value of the atoms they are linked to (1.5 times for methyl groups). Details of the data quality and a summary of the residual values of the refinements are listed in table S2. Tables S3–S8 provide all bond lengths and angles for the obtained structures (Supporting Information).

Preparation of 7: Phosphinine selenide **6** (32 mg, 0.1 mmol) was dissolved in dichloromethane (2 mL) at $T = -30$ °C. Subsequently, 1,4-TFDIB (40 mg, 0.1 mmol) was added to the solution. Another 2 mL of *n*-pentane was layered on the dichloromethane solution. The co-crystalline adduct **7** was obtained after the solution was evaporation at $T = -30$ °C. ^{1}H NMR (400 MHz, C_6D_6) δ 7.47 (dd, $^3J_{H,P} = 42.7$, $^3J_{H,H} = 8.1$ Hz, 2H, *meta-H*), 6.64 (q, $^4J_{H,P} = 8.0$ Hz, 1H, *para-H*), 0.43 (s, 18H, –Si*Me*$_3$) ppm. ^{13}C{^{1}H} NMR (101 MHz, CD_2Cl_2) δ 148.6–147.8 (m, $C_6F_4I_2$), 146.1 (d, $^3J_{C,P} = 15.1$ Hz, *meta-C*-C_5H_3P), 145.5 (d, $^4J_{C,P} = 14.6$ Hz, *para-C*-C_5H_3P), 120.0 (d, $^2J_{C,P} = 52.2$ Hz, *ortho-C*-C_5H_3P), 73.5–73.2 (m, $C_6F_4I_2$), −1.0 (d, $J = 2.8$ Hz, –Si*Me*$_3$) ppm. ^{31}P NMR (162 MHz, CD_2Cl_2) δ 168.39 (td, $J_{H,P} = 43.1$, 7.6 Hz, $^1J_{P–Se} = 883.5$ Hz) ppm. ^{31}P{^{1}H} NMR (162 MHz, C_6D_6) δ 170.3 (s, $^1J_{P–Se} = 883.5$ Hz) ppm. ^{19}F NMR (377 MHz, CD_2Cl_2) δ −114.6 ppm. ^{77}Se {^{1}H} NMR (76 MHz, CD_2Cl_2) δ −28.0 (d, $^1J_{P–Se} = 878.8$ Hz).

Preparation of 8: Phosphinine selenide **6** (32 mg, 0.1 mmol) was dissolved in dichloromethane (1 mL) at $T = -30$ °C and I_2 (25 mg, 0.1 mmol) was added to the solution. The dichloromethane solution was stored in the freezer at $T = -30$ °C and red crystals were obtained after the solvent slowly evaporated. Product yield: 92%

(0.09 mmol, 51.6 mg). ^{1}H NMR (600 MHz, CD_2Cl_2) δ 7.94 (dd, $^{1}J_{H,P}$ = 44.4, $^{2}J_{H,H}$ = 8.1 Hz, 2H, *meta-H*), 7.27 (q, $^{3}J_{H,P}$ = 8.2 Hz, 1H, *para-H*), 0.49 (s, 18H, −Si*Me*$_3$) ppm. ^{13}C{^{1}H} NMR (151 MHz, CD_2Cl_2) δ 148.5 (d, $^{3}J_{C,P}$ = 13.0 Hz, *para-C*), 146.8 (d, $^{2}J_{C,P}$ = 16.4 Hz, *C2*, *meta-C*), 122.4 (d, $^{1}J_{C,P}$ = 54.5 Hz, *ortho-C*), −0.7 (d, *J* = 2.9 Hz, −Si*Me*$_3$) ppm. ^{31}P{^{1}H} NMR (243 MHz, CD_2Cl_2) δ 162.0 (s, $^{1}J_{P-Se}$ = 832.5 Hz) ppm. HR-ESI MS (m/z): 573.5846 (Calculated: 573.8169) $[M]^+$.

Synthesis of KSeCN: Phosphinine selenide **6** (32 mg, 0.1 mmol) was dissolved in acetonitrile (1 mL) and KCN (6.5 mg, 0.1 mmol) was added to the solution at room temperature. After stirring for 2 hours, the solvent was slowly evaporated to afford dark red crystals in quantitative yield. (14 mg). The free phosphinine **6** could be detected as a viscous oil at the bottom of the vial.

Acknowledgements

Funding by Freie Universität Berlin, the Deutsche Forschungsgemeinschaft DFG (Project-Nr 2100302201) as well as the China Scholarship Council is gratefully acknowledged. Open Access funding enabled and organized by Projekt DEAL.

Conflict of Interest

The authors declare no conflict of interest.

Data Availability Statement

The data that support the findings of this study are available from the corresponding author upon reasonable request.

Keywords: co-crystals · noncovalent interactions · phosphorus · σ-holes · selenium

[1] For recent examples, see a) M. L. Kelty, A. J. McNeece, J. W. Kurutz, A. S. Filatov, J. S. Anderson, *Chem. Sci.* **2022**, *13*, 4377–4387; b) W. P. Teh, D. C. Obenschain, B. M. Black, F. E. Michael, *J. Am. Chem. Soc.* **2020**, *142*, 16716–16722; c) T. Zheng, J. R. Tabor, Z. L. Stein, F. E. Michael, *Org. Lett.* **2018**, *20*, 6975–6978; d) S. Konishi, T. Iwai, M. Sawamura, *Organometallics* **2018**, *37*, 1876–1883; e) M. J. Poller, N. Burford, K. Karaghiosoff, *Chem. Eur. J.* **2018**, *24*, 85–88.
[2] T. Murai, T. Kimura, *Curr. Org. Chem.* **2006**, *10*, 1963–1973.
[3] a) M. Bollmark, J. Stawinski, *Chem. Commun.* **2001**, *8*, 771–772; b) R. Rodríguez, H. Liu, *J. Am. Chem. Soc.* **2012**, *134*, 1400–1403.
[4] J. A. Gillespie, E. Zuidema, P. W. Van Leeuwen, P. C. Kamer, *Phosphorus (III) ligands in homogeneous catalysis: design and synthesis*, (Eds: P. C. Kamer, P. W. Van Leeuwen), John Wiley & Sons, **2012**, Ch. 1.
[5] a) H. D. Arman, E. R. Rafferty, C. A. Bayse, W. T. Pennington, *Cryst. Growth Des.* **2012**, *12*, 4315–4323; b) A. J. Peloquin, C. D. McMillen, S. T. Iacano, W. T. Pennington, *ChemPlusChem* **2021**, *86*, 549–557.
[6] a) H. Wang, W. Wang, W. J. Jin, *Chem. Rev.* **2016**, *116*, 5072–5104; b) T. Sakurai, M. Sundaralingam, G. Jeffrey, *Acta Crystallogr.* **1963**, *16*, 354–363.
[7] A. Hasija, D. Chopra, *Cryst. Growth Des.* **2020**, *20*, 6272–6282.
[8] K. Lisac, F. Topić, M. Arhangelskis, S. Cepić, P. A. Julien, C. W. Nickels, A. J. Morris, T. Friščić, D. Cinčić, *Nat. Commun.* **2019**, *10*, 1–10.
[9] R. Bhowal, S. Biswas, D. P. A. Saseendran, A. L. Koner, D. Chopra, *CrystEngComm* **2019**, *21*, 1940–1947.
[10] T. Salzillo, M. Masino, G. Kociok-Köhn, D. Di Nuzzo, E. Venuti, R. G. Della Valle, D. Vanossi, C. Fontanesi, A. Girlando, A. Brillante, *Cryst. Growth Des.* **2016**, *16*, 3028–3036.
[11] a) R. Lee, A. J. Firbank, M. R. Probert, J. W. Steed, *Cryst. Growth Des.* **2016**, *16*, 4005–4011; b) M. Singh, D. Chopra, *Cryst. Growth Des.* **2018**, *18*, 6670–6680.
[12] R. A. Zingaro, E. A. Meyers, *Inorg. Chem.* **1962**, *1*, 771–774.
[13] S. M. Godfrey, S. L. Jackson, C. A. McAuliffe, R. G. Pritchard, *J. Chem. Soc. Dalton Trans.* **1997**, 4499–4502.
[14] a) Y. Feng, D. Rainteau, C. Chachaty, Z. W. Yu, C. Wolf, P. J. Quinn, *Biophys. J.* **2004**, *86*, 2208–2217; b) F. G. Wu, N. N. Wang, Z. W. Yu, *Langmuir* **2009**, *25*, 13394–13401.
[15] X. Guo, X. An, Q. Li, *J. Phys. Chem. A* **2015**, *119*, 3518–3527.
[16] F. Wossidlo, D. S. Frost, J. Lin, N. T. Coles, K. Klimov, M. Weber, T. Böttcher, C. Müller, *Chem. Eur. J.* **2021**, *27*, 12788–12795.
[17] A. Moores, T. Cantat, L. Ricard, N. Mézailles, P. Le Floch, *New J. Chem.* **2007**, *31*, 1493–1498.
[18] S. Nyburg, C. Faerman, *Acta Crystallogr. Sect. B* **1985**, *41*, 274–279.
[19] A. Shlyaykher, M. Ehmann, A. J. Karttunen, F. Tambornino, CCDC 2080510: Experimental Crystal Structure Determination, **2021**, DOI: 10.5517/ccdc.csd.cc27ty78.
[20] G. M. Sheldrick, *Acta Crystallogr. Sect. A* **2015**, *71*, 3–8.
[21] G. M. Sheldrick, *Acta Crystallogr. Sect. C* **2015**, *71*, 3–8.
[22] P. Müller, *Crystallogr. Rev.* **2009**, *15*, 57–83.
[23] O. v. Dolomanov, L. J. Bourhis, R. J. Gildea, J. A. K. Howard, H. Puschmann, *J. Appl. Crystallogr.* **2009**, *42*, 339–341.

Manuscript received: August 18, 2022
Revised manuscript received: September 20, 2022
Accepted manuscript online: September 30, 2022